European Geosciences Union General Assembly 2014, EGU 2014

Turbulence characteristics in offshore wind farms from LES simulations of Lillgrund wind farm

Wolf-Gerrit Früh[a]*, Angus C.W. Creech[b], A. Eoghan Maguire[c]

[a]*School of Engineering and Physical Sciences, Heriot-Watt University, Edinburgh, Scotland, UK*
[b]*School of Engineering, University of Edinburgh, Edinburgh EH9 3JL, Scotland, UK*
[c]*Vattenfall United Kingdom, The Tun, Holyrood Road, Edinburgh, Scotland, UK*

Abstract

The effect of wind turbine wakes in large offshore wind energy arrays can be a substantial factor in affecting the performance of turbines inside the array. Turbulent mixing plays a key role in the wake recovery, having a significant effect on the length over which the wake is strong enough to affect the performance of other turbines significantly. We highlight how turbulence affects wind turbine wakes using results from LES simulations of Lillgrund offshore wind farm in the context of SCADA data selected to mirror the wind conditions simulated. The analysis here concentrated on temporal spectra of wind velocities measured by the turbine's nacelle anemometer and calculated at the turbine locations in the computational model. The effect of the wind turbine rotor on the downstream flow is quantified by analysing the change in spectral features of turbines within the wind farm compared to turbines at the side of the farm exposed to the wind.

Keywords: wind turbine ; wake ; turbulence.

1. Introduction

With new offshore wind farms being built at an increasing rate and scale, the financial implications of losing out on potential electricity production due to turbine wakes adversely affecting downstream turbines in the wind farm are significant. It has been shown that turbines within the wind farm may produce as little as 30% of their potential

---

* Corresponding author. Tel.: +44-131-451-4374; fax: +44-131-451-3129.
  E-mail address: w.g.fruh@hw.ac.uk

when they are in the wake of another turbine [1] and that the free-stream turbulence affects the wake recovery substantially [2]. One observation from the wind farm investigated here was that the second turbine in a row was performing worst of all [1,3] which suggested that a complex interaction of the free-stream turbulence and the turbulence created by the turbine rotors may lead to a slow wake recovery after the front turbine, but faster recovery further into the array. The aim of this paper is to investigate some turbulence characteristics of the air flow at the locations of the turbines using measured and simulated nacelle wind speeds data.

1.1. Lillgrund wind farm

Lillgrund offshore wind farm is located 7 km south of the Øresund bridge between Copenhagen in Denmark and Malmö in Sweden and has been operated by Vattenfall Vindkraft AB since December 2007 [4].

The array consists of 48 turbines, each with a rotor diameter of $D = 93$ m and a hub height of 65 m, in a regular lattice-type array as shown in Fig. 1 (a) where each turbine is given a number as well as a grid-name using column letters A to H and row numbers 1 to 8. The turbines are close to each other, with a spacing of $4.3D = 400$ m in the prevailing wind direction, 223°), and $3.3D = 307$ m in the transverse. Overall, the extent of the wind farm is up to 2.9 km in the prevailing wind direction and 2.25 km across, covering a total area of around 6 km^2.

The analysis data set was derived from the output of turbine diagnostics from the SCADA (supervisory control and data acquisition) system at an interval of 1 minute covering a period of 323 days, starting in January 2008 when all turbines were connected to the system.

2. Methodology

2.1. The computational model

The Computational Fluid Dynamics (CFD) solver used in these simulations was the hr-adaptive finite-element solver Fluidity, with the Wall-adapting Local Eddy (WALE) subgrid turbulence model [5], a variant of Large Eddy Simulation (LES).

The three-dimensional computational domain had a square area of 8.1 km by 8.1 km, and a height of 600 m, as shown in Fig. 1b. The wind farm was positioned such that the first turbine was 2 km from the inlet, allowing turbulence to develop fully before encountering the wind farm. The orientation of the domain was kept constant such that one side was always specified with a prescribed inlet velocity profile consistent with a neutral atmosphere frequently found at Lillgrund [6], superimposed on which atmospheric turbulence was introduced using the Synthetic Eddy method [7].
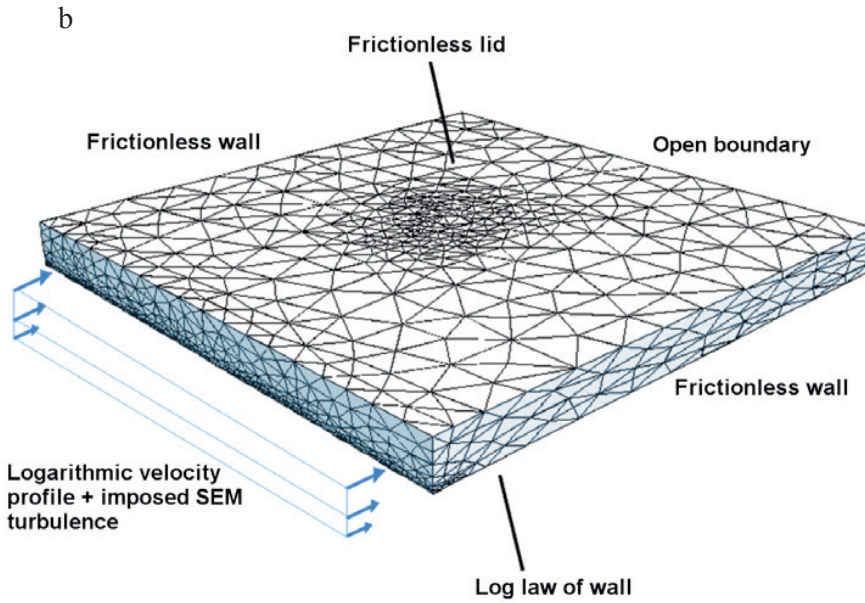
a

b
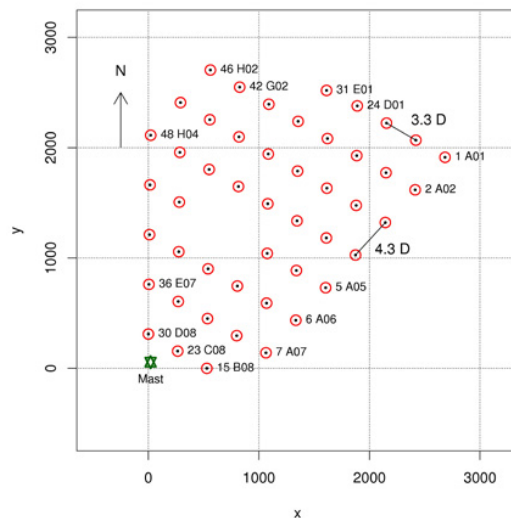
Fig. 1. (a) Layout of Lillgrund wind farm and (b) Illustration of the computational domain.
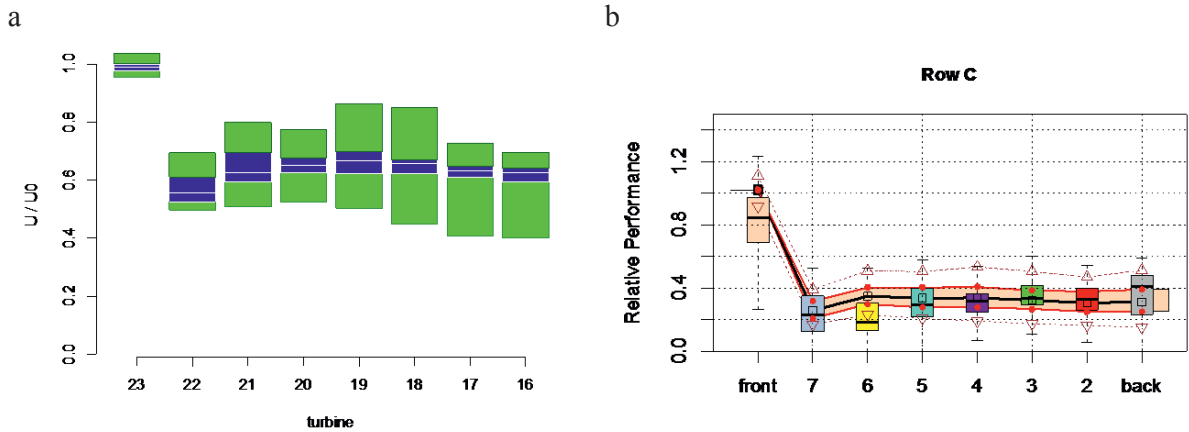
a   b

Fig. 2. (a) Velocity measured at turbines in row C and (b) effect of turbine wakes on performance of downstream turbines, both for a wind direction of 223°.

The turbines were incorporated into the CFD domain using a variant of the actuator disc method, which featured both, a torque-controlled generator and active blade pitching. The interaction between the fluid and the turbine was achieved through the lift and drag coefficients from the turbine blades, with blade solidity distributed uniformly in the azimuthal direction, and spread with a Gaussian function in the streamwise direction within the turbine volume. Additionally, some turbulence was generated, especially in the tip region [2].

Far away from the turbines the resolution was 75 m in the horizontal and at least 25 m in the vertical, whilst nearer the turbines, the resolution was a maximum of 5 m both horizontally and vertically. To simulate different wind directions, the entire wind farm was rotated within the fixed fluid domain.

2.2. Model configuration

Based on a previous assessment of the wind farm performance [1, 8], the SCADA data analysis was restricted to a wind speed band well within the cut-in wind speed and the rated wind speed, namely between 5.5 and 11 m/s, and the CFD model used a nominal wind speed of 10 m/s at hub height to specify the inflow conditions with a vertical profile consistent with a neutral atmosphere. This ensured that the turbines would not reach their rated power but that even those within a strong wake would still be operating.

After an initial spin-up of the model without active turbines lasting for 2000 s simulation time, the turbines were activated and allowed to reach stable operating conditions, as monitored by the power output from the turbines. Typically, the turbine models had reached that level after around 400 to 600 s of model time. The actual model results were then obtained from continuing the simulation for a further 600 s. The set of simulations covered eight wind directions from 198° to 236°. The material presented here is primarily for the wind direction of 223°, when the wind direction is fully aligned with the turbine column, and 229° when the second turbine is partially shaded by the front turbine.

3. Results

In this section, we first illustrate the observations from the SCADA system to provide the framework for the computational results. After presenting the results in terms of turbulence intensity, the findings are refined by a spectral analysis of the streamwise velocity component.
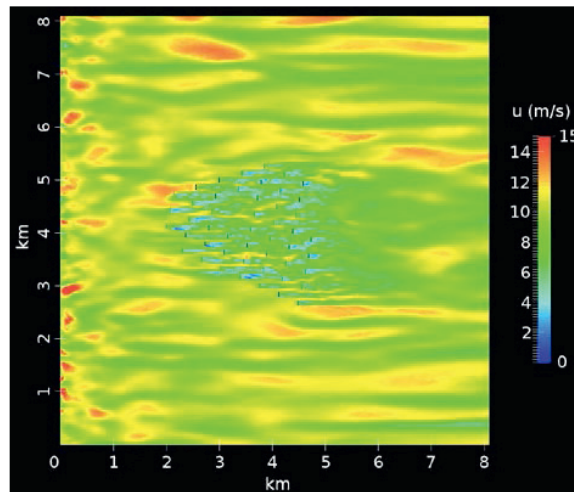

Fig. 3. Snapshot of the streamwise velocity field at hub height at the end of the simultion for the wind direction of 198°.

3.1. SCADA results

Fig. 2a shows the range of wind speeds at the turbines in row C in the centre of the wind farm when the wind direction is fully aligned with that row in a form of boxes showing the quartiles of the observations from the SCADA system. The second turbine has the lowest median velocity although turbines further downstream may have a larger range. This behaviour is mirrored by the power output from those turbines in Fig. 2b where the shaded background corresponds to the observations from the SCADA system and the box-and-whisker plots show the CFD results. One can also see in Fig. 2a that the velocity range is smallest for the front turbines and increases deeper into the turbine array.

3.2. Computational results

A typical instantaneous snapshot of the streamwise velocity magnitude in a horizontal slice is shown in Fig. 3 where the left side is the inlet with the prescribed velocity profile and synthetic eddies to lead to a typical turbulence intensity at the wind farm location. The first 1000 m are an entrance section where the generated eddies break up into a typical spectrum and are then advected through the domain. One can see a few eddies and streaks persisting throughout the domain, with some leading to jetting within the domain but one can also see the wakes behind individual turbines (with blue and turquoise colours) and an extended wind farm wake persisting up to the outlet on the right.

3.3. Turbulence intensity

From the velocity time series of the equilibrated final 10 minutes of integration, sampled every 0.5 s, the turbulence intensity was calculated as $TI = \sigma(u) / U_0$ where U_0 is the upstream wind speed at hub height. These computational results, shown as a box-and-whiskers plot for all eight wind directions investigated in Fig. 4a, are largely consistent with the SCADA data in that the turbulence intensity is smallest at the front turbine, reaches a maximum within the wind farm and then slightly reduces towards the rear of the of the array. It has to be born in mind that this includes cases where the turbine C07 is fully exposed to the free stream as well as those where it is fully shaded by C08, which explains the large range of turbulence intensities found for C07 across this wind direction sector. To resolve the variation in the turbulence intensity for each wind direction, we represent the turbulence intensity for each turbine in row C (in the columns) against the wind directions simulated (in the rows) in Fig. 4b. There we see a fairly uniformly low turbulence level in the front turbine, but also a *TI* maximum in second row when this turbine is partially shaded and a low *TI* in that turbine when it is either fully exposed or fully shaded.

This suggests that turbulence generation at the blade tips and subsequent mixing at the edge of the expanding wake with the surrounding air is a key process in organising the evolution of the wake. In particular, the wake recovery of a turbine's wake and consequent power output at a downstream turbine is strongly affected by the inflow conditions into the upstream turbine. The wake of turbine C08 recovers slowly as its rotor is exposed to low-turbulence flow, and the turbulence is concentrated at the perimeter of the wake, only gradually mixing towards the wake's centre. Hence, turbine C07, when fully shaded by C08, experiences a relatively deep wake with only slightly elevated turbulence. The combination of the wake from C07 within C08 then provides sufficient turbulence levels and turbulent mixing to recover that combined wake faster, leading to a higher power output at C06 as well as a higher turbulence intensity at that turbine. In contrast, when C07 is only partially shaded, its rotor intersects with the perimeter of C08's wake with the result that it experiences a high turbulence intensity as well as spatially highly-variable wind speeds, leading to power output between that of the fully shaded and fully exposed cases. In addition to the higher turbulence level, the turbine blades will also experience laterally varying loading.

3.4. Spectra

The turbulence intensity provides a good but fairly blunt measure of the flow characteristics. To understand the processes better one can use spectra of the velocity components or of the kinetic energy to identify length scales or time scales which play an active role in the flow dynamics. With an available sampling rate of 1 min^{-1}, the SCADA data are insufficiently sampled for a spectral analysis but the CFD results, sampled at 2 Hz are sufficiently sampled to access the time scales of interest for wind turbines.

Fig. 5 overlays the temporal spectra of the streamwise velocity for the first four turbines in row C (C08 to C05) in (a) for the wind direction where they all are fully shaded by the front turbine (223°) and, in (b), for the case where C07 is partially shaded by C08. On the whole they all show similar spectra, with a relatively flat part at the low frequencies below ≈0.1 Hz, a decay largely consistent with $\propto f$ −1 in the frequ Hz, and a high-frequency decay consistent with $\propto f^{-5/3}$. In the fully shaded situation, there is very little difference between the four spectra with no clear difference between those for C08 and C07, but a slightly extended low-frequency shelf (from ≈0.01 to ≈0.02 Hz) and very slightly enhanced variability for C06 and C05 at frequencies

around 0.05 Hz and for C05 alone at around 0.025 Hz. In contrast, when the turbines are not fully aligned, the low-frequency plateau is also extended for C07, and C06 and C05 show enhanced variability clearly in the frequency range from 0.02 to 0.05 Hz.
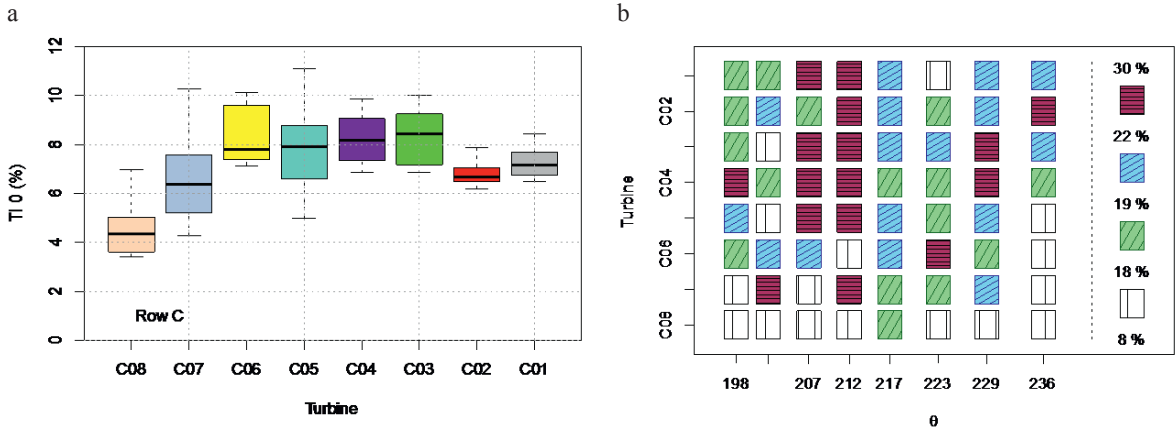

Fig. 4. (a) Standard deviation of velocity in row C; (b) Level plot of turbulence intensity at row C for all wind directions.
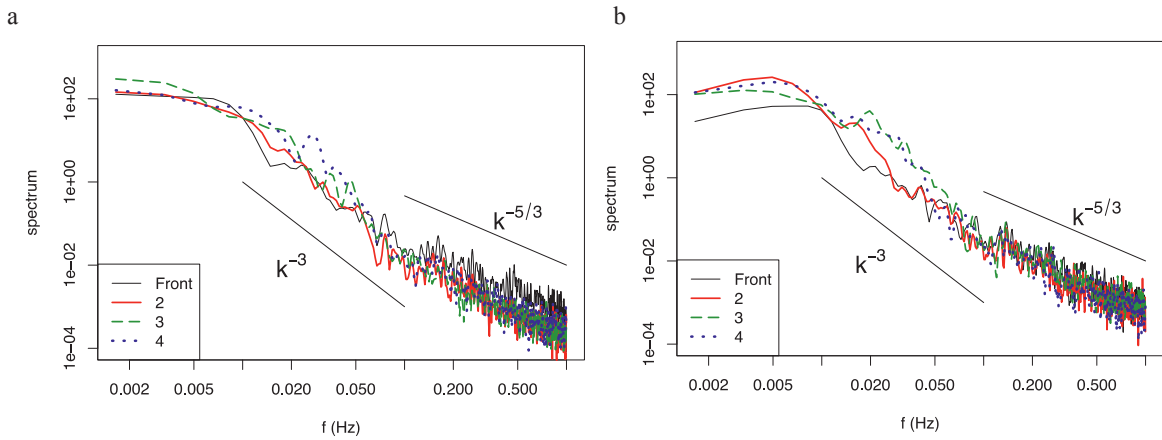

Fig. 5. Spectrum of streamwise velocity at the first four turbines, (a) at a wind direction of 223° when all turbines are fully shaded by the front turbine the front turbine, and (b) at a wind direction of 229° when the second turbine is only partially shaded by the front turbine.
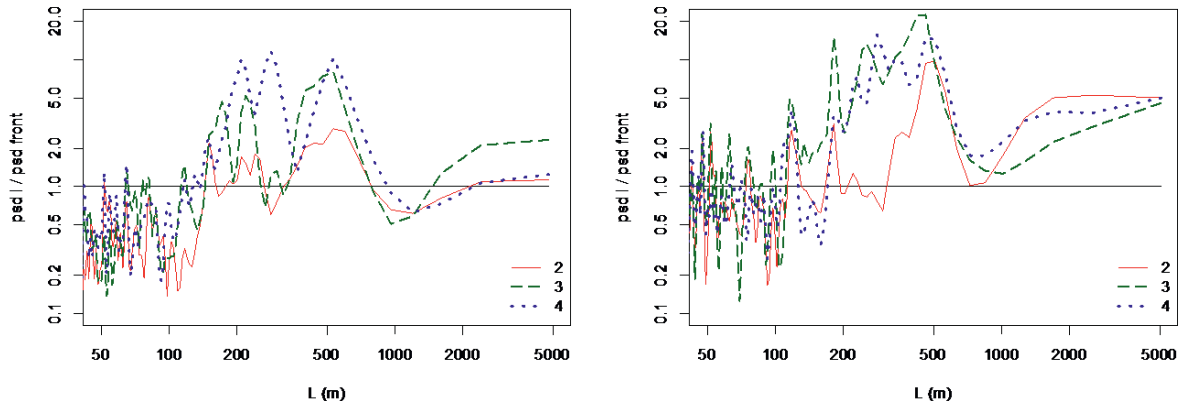
Fig. 6. Ratio of the Spectra of second to forth turbines over that of the front turbine, with the horizontal axis rescaled to equivalent length scales, (a) at a wind direction of 223° when the all other turbines are fully shaded by the front turbine, and (b) at a wind direction of $229° when the second turbine is only partially shaded by the front turbine.

To draw out these differences, the ratio of the spectral amplitude for a turbine at each frequency over that at the front turbine was calculated. To also get a feeling for the length scales of flow with a mean velocity transporting the fluctuations, the frequencies were transformed to equivalent length scales by $L = U_0/f$. The results of this comparison and transformation are shown in Fig. 6 for the same cases as in Fig. 5. They highlight for 223° in Fig. 6(a) that the second turbine (C07, solid red line) experiences little change in the spectral characteristics of the flow while the third (C06, dash-double-dotted green line) sees enhancement at the length scales around 200 and 500 m and a further enhancement in fourth row (C05, purple dash-dotted line) at around 300 m. At the wind direction of 229° in Fig. 6b, the second turbine experiences full enhancement at the length scale of 500 m which then extends down to 200 m for the third turbine with no obvious further change for the fourth turbine.

4. Conclusions

We have demonstrated that high-resolution large-eddy simulation of wind farms using appropriate turbine representations can be used to investigate the link between atmospheric and turbine-generated turbulence and their effect on wake recovery and turbine performance. The model results highlight the link between turbulence intensity, wake recovery and wind farm performance, suggesting that the intersection or interaction of successive turbine wakes is a key factor in determining the wake decay. A better quantitative understanding of this process will help to refine engineering wake models to improve the representation of multiple wakes in a large turbine array. The spectral analysis of the wind speed time series at the turbine location has shown that the increased turbulence intensity can be associated with distinct time or length scales which are at length scales of the turbine spacing. To substantiate this, the next analysis step is a spatial spectral analysis of the full flow field.

Acknowledgements

References

[1] Creech, ACW, Früh, W-G, Maguire, AE. Full-scale simulations of a wind farm using large eddy simulation and a torque-controlled actuator disc model. Surveys in Geophysics submitted.

[2] Creech, ACW, Früh, W-G, Clive, P. Actuator volumes and hr-adaptive methods for 3D simulation of wind turbine wakes and performance. Wind Energy 2012;15(6):847-863.

[3] Creech, ACW, Früh, W-G, Maguire, AE. High-resolution CFD modelling of Lillgrund wind farm. In: International Conference on Renewable Energies and Power Quality (ICREPQ'13); vol. 11. Renewable Energy and Power Quality Journal; 2013.

[4] Jeppsson, J, Larsen, PE, Larsson, Å. Technical description Lillgrund wind power plant. Tech. Rep. 2.1 Lillgrund Pilot Project; Vattenfall Vind-kraft AB; 2008.

[5] Nicoud, F, Ducros, F. Subgrid-scale stress modelling based on the square of the velocity gradient tensor. Flow, Turbulence and Combustion 1999;62:183-200.

[6] Bergström, H.. Meteorological conditions at Lillgrund. Tech. Rep. 6 2 LG Pilot Report 21858-1; Vattenfall Vindkraft AB; 2009.

[7] Jarrin, N, Benhamadouche, S, Laurence, D, Prosser, R. A synthetic- eddy-method for generating inflow conditions for large-eddy simulations. Int Journal of Heat Fluid Flows 2006;27:585-593.

[8] Dahlberg, JÅ. Assesment of the Lillgrund windfarm: Power performance, Wake effects. Tech. Rep. 6.1 Lillgrund Pilot Project; Vattenfall Vindkraft AB; 2009.